Journal of Photochemistry and Photobiology A: Chemistry 220 (2011) 113–123

Contents lists available at ScienceDirect

Journal of Photochemistry and Photobiology A: Chemistry

journal homepage: www.elsevier.com/locate/jphotochem

Nanoparticulate silver coated-titania thin films—Photo-oxidative destruction of stearic acid under different light sources and antimicrobial effects under hospital lighting conditions

Charles W. Dunnill [a], Kristopher Page [a], Zoie A. Aiken [b], Sacha Noimark [a], Geoffrey Hyett [a], Andreas Kafizas [a], Jonathan Pratten [b], Michael Wilson [b], Ivan P. Parkin [a,*]

[a] Centre for Materials Chemistry, Department of Chemistry, University College London, 20 Gordon Street, London WC1H 0AJ, United Kingdom
[b] Division of Microbial Diseases, Eastman Dental Institute, University College London, 256 Grays Inn Road, London WC1X 8LD, United Kingdom

ARTICLE INFO

Article history:
Received 10 December 2010
Received in revised form 3 March 2011
Accepted 1 April 2011
Available online 12 April 2011

Keywords:
Visible light photocatalysis
Antimicrobial
Stearic acid
Thin film
Photo-assisted silver nanoparticles
MRSA
E. coli

ABSTRACT

Antimicrobial films containing silver nanoparticles on a titania substrate were prepared and shown to have marked visible light photocatalytic properties. The films could be transformed from purple (silver oxide) to orange (silver) by 254 nm, 365 nm or white light radiation and the process reversed when the films were stored in air and in the dark. The films were characterized by XRD, Raman, AFM, SEM, EDX, UV–Vis spectroscopy and XPS as well as tested for functionality using a range of techniques including water contact angle measurement, the photo-destruction of stearic acid to a range of light sources and antimicrobial activity against MRSA and *Escherichia coli* bacteria under hospital lighting conditions. XRD and Raman indicated that the films were anatase, X-ray photoelectron measurements confirmed the presence of silver loading on the titania surface and EDX showed silver doping in the TiO_2 layer. There appears to be an interaction between the phonon resonance of the silver nanoparticles and the band onset of the titania leading to significant visible light photo-oxidation of stearic acid as well as visible light induced superhydrophilicity. Samples were tested for photo-degradation of stearic acid under three different lighting conditions: UVA – 365 nm, white light (commonly found in UK hospitals) and UVA filtered white light. The Ag oxide-titania films were seen to be active photocatalysts under visible light conditions as well as displaying white light induced superhydrophilicity. These surfaces demonstrated a 99.996% reduction in the number of viable *E. coli* bacteria due to the silver ion presence and a 99.99% reduction in the number of MRSA bacteria due to the enhanced photocatalysis in a double pronged approach to antimicrobial mechanisms consisting of a synergistic relationship between the photocatalyst (TiO_2) and the surface bound silver nanoparticles.

© 2011 Elsevier B.V. All rights reserved.

1. Introduction

Titanium dioxide (TiO_2) thin films are chemically stable, possess high refractive index, have excellent transmission in the infra red and visible regions and are the most researched photocatalyst [1–7]. They have found wide-spread commercial applications for bathroom tiles, paving slabs, deodorizers in underground stations and as self-cleaning windows such as Pilkington Activ™ [8]. Titanium dioxide films have the potential to provide clean, sustainable and renewable energy as under the action of sunlight they can form a working photodiode that can split water into oxygen and hydrogen fuel [9–11]. These extraordinary functional properties arise because titanium dioxide under UV-light generates a mobile electron–hole pair that can migrate to the surface where photo-generated holes oxidize any organic species and photo-generated electrons reduce oxygen to water mediated by oxygen radical formations [1]. This enables the surface to photo-mineralize organic material sensitized by the semiconductor, as well as making the surface superhydrophilic.

Titanium dioxide is photo-stable and is exceptionally well adhered to a range of ceramic substrates as well as being impervious to the majority of chemical attacks. One limitation of titanium dioxide is that it requires sub 385 nm radiation (ca. 2% of the incident suns energy at sea level [12]) to function. A major research effort has been directed to shifting the band onset into the visible. This will enable better solar harvesting which could improve the overall effectiveness of the photocatalyst and furthermore enable a visible light activated surface that has potential in a healthcare setting.

Healthcare-associated infections remain a reason for major concern in western hospitals. The Center for Disease Control (CDC)

* Corresponding author. Tel.: +44 207 679 4669.
E-mail address: i.p.parkin@ucl.ac.uk (I.P. Parkin).

1010-6030/$ – see front matter © 2011 Elsevier B.V. All rights reserved.
doi:10.1016/j.jphotochem.2011.04.001

has recently reported that healthcare-associated infections are in the top ten leading causes of death in the United States [13,14]. An estimated 1.7 million infections annually are acquired in the healthcare environment and these result in 99,000 deaths in America alone [15,16]. Figures for the UK are proportionally similar with healthcare-associated bacterial infections recorded as a "significant factor" in over 7500 death certificates in 2008 [17]. It is estimated that healthcare-associated infections cost the UK tax payer ~£1bn pa [18].

Photocatalytic films have received much attention in the literature for their ability to destroy bacteria such as Methicillin-resistant *Staphylococcus aureus* (MRSA) and *Escherichia coli* (*E. coli*) which are major contributors to hospital acquired infections [19–22]. The mechanism by which semiconductors thin films act as antimicrobial coatings follows analogously from research on self-cleaning films [2,23–25].

One important, yet hard to achieve feature of a photo-activated antimicrobial thin film coating for application within a healthcare environment is the ability to photo-degrade bacteria using indoor lighting conditions. Demonstrating visible light photocatalysis on a range of organic media and bacteria is therefore essential. Many researchers are investigating visible light photocatalysts using titania as a base and modifying the structure using dopants; such as metals [1,26,27], including silver [28–32] and anions such as nitrogen [24,33–39], carbon [19] and sulfur [23,40–43]. Many comparative reviews are available in this area [1–3,20,21,44], yet no consensus for the most effective dopant for visible light photocatalysis has yet been found. The use of such coatings for an antimicrobial application has been demonstrated with variable success and is yet to be unambiguously proven using visible light [25,45–47].

Researchers have also been investigating the use of silver ions in the search for antimicrobial surfaces. Silver ions can migrate from the antimicrobial material surface into microbes with a high level of toxicity thus effecting antimicrobial properties [21,48,49]. A range of commercial products exist based on silver bactericidal effects including ventilator tubing, catheters, clothing and surfaces [20]. The use of silver ions, though popular, may have serious cytotoxic activity on host cells and inhibit the healing process, as shown by a recent review into the use of silver compounds in the treatment of burns [50].

In this paper a synergistic approach to surfaces exhibiting antimicrobial activity due to both the inherent toxicity of silver ions and photocatalysis under hospital lighting conditions using a titania photocatalyst loaded with surface bound silver nanoparticles is shown. The functional films were prepared using a sol–gel method to coat glass microscope slides with the anatase polymorph of titania before silver nanoparticles were generated on the surface by UV photo-assisted reduction of silver nitrate solution. The films showed marked photochromism and could be shuttled between silver oxide (purple) and silver (orange) using different light sources and oxygen/air. From this work we show unambiguously that the Ag-TiO_2 films are active visible light photocatalysts. The films were also shown to be exceptionally potent at killing *E. coli* and MRSA; organisms implicated in a significant number of hospital acquired infections. Notably we found that the *E. coli* were killed directly by the silver loading whereas the MRSA showed some silver resistance and was more susceptible to the combination of light and silver induced kill.

2. Methods

Thin films of TiO_2 were prepared by a sol–gel preparation and then post treated using silver nitrate to adhere silver nanoparticles to the surface of the titania film. A dip-coating apparatus was used to withdraw the substrate from the sol at a steady rate of 120 cm min^{-1}. The deposited xerogel films were not mechanically stable, and required sintering in order to properly adhere to the substrate and to become crystalline. Hence, all films were annealed in a furnace at 500 °C for 1 h (heating rate 10 °C min^{-1}, cooling rate 60 °C min^{-1}).

To prepare the sol, acetylacetone (2.5246 g, 0.02526 mol, Sigma Aldrich, 99+%) was dissolved in butan-1-ol (32 cm^3, 0.35 mol, Sigma Aldrich, 99.4%) forming a clear and colourless solution. To this solution, titanium n-butoxide (17.50 g, 0.05 mol, Fluka, 97.0%) was added. The solution was stirred vigorously for an hour, before distilled water (3.64 ml, 0.20 mol), dissolved in isopropanol (9.05 g, 0.15 mol, Fisher Scientific, analytical grade) was added. The sol remained clear, but deepened in yellow colouration and was stirred for a further hour. Finally acetonitrile (1.66 g, 0.04 mol, Fisons Scientific equipment 99% min), was added to the solution, which was then stirred for a final hour. The sol was allowed to age overnight before being used for dip-coating. Samples of TiO_2 were prepared with two dips in the sol retracting at a rate of 120 cm min^{-1} with the xerogel allowed to dry between each dip. The slides were heated in a muffle furnace to 500 °C for 1 h (10 °C min^{-1}) and allowed to cool slowly. Single cavity ground glass slides (Jencons) were used as the substrate. Half of these slides were put aside in a dark drawer and are referred to as sample TiO_2.

Half of the slides were dipped in silver nitrate solution in methanol (5×10^{-3} M made up from $AgNO_3$, Fisher Scientific) for 30 s and withdrawn at 120 cm·min^{-1} before being exposed to UV radiation 254 nm for 1 h. Photodeposition occurs quickly (<30 min) however an excess of time was used to remove the time of irradiation as a variable and ensure that the films were fully clean and activated prior to initial characterization. These microscope slides are referred to as sample Ag-TiO_2.

2.1. Characterization

X-ray diffraction was performed using a Bruker-Axs D8 (GADDS) diffractometer, utilizing a large 2D area detector and a Cu X-ray source, monochromated ($K_{\alpha1}$ and $K_{\alpha2}$) fitted with a Gorbel mirror. The instrumental setup allowed 34° in both θ and ω with a 0.01° resolution and 3–4 mm^2 of sample surface illuminated at any one time. Multiple Debye–Scherrer cones were recorded simultaneously by the area detector with two sections covering the 65° 2θ range. The Debye–Scherrer cones, once collected were integrated along ω to produce standard diffraction patterns of degrees 2θ against intensity. Scan data was collected for 1000 s periods to give sufficiently resolved peaks for indexing. Raman was conducted using a Renishaw inVia Raman microscope, between 100 and 1000 cm^{-1} Raman shift, and UV–visible–NIR; transmission and reflectance measurements were achieved using a Perkin Elmer λ950. Scanning electron microscopy was performed using secondary electron imaging on a JEOL 6301 field emission instrument. Atomic force microscopy (AFM) was conducted on a Veeco Dimension 3100 in air using a tapping operating mode and a silicon tipped cantilever. Sample areas of 1 μm × 1 μm were analyzed for a plain titania and surface nanoparticle silver deposited titania sample.

Samples were analyzed by XPS using the Kratos AXIS ULTRA with a mono-chromated Al K_α X-ray source (1486.6 eV) operated at 10 mA emission current and 120 kV anode potential −100 W at Nottingham University. Wide scans were run for 10 min and high resolution scans for 5 min on two to three areas per sample. The ULTRA was used in FAT (fixed analyzer transmission) mode, with pass energy of 80 eV for wide scans and pass energy 20 eV for high resolution scans. The magnetic immersion lens system allowed the area of analysis to be defined by apertures, the 'slot' aperture of 300 μm × 700 μm was used for all wide/survey scans and high resolution scans. The take-off angle for the photoelectron analyzer is 90° and acceptance angle of 30° (in magnetic lens modes).

2.2. Functional testing

The self-cleaning properties of the thin films were assessed using water contact angle measurements, the photo-destruction of stearic acid and the antimicrobial effect on *E. coli* and MRSA bacteria.

Water contact angle measurements were taken as an average of 5 measurements on a 8.6 μl deionised water droplet using FTA 1000 droplet analyzer. The drop was formed and dispensed by gravity from the tip of a gauge 27 needle.

To measure the photo-oxidation of a stearic acid overlayer, duplicate samples were housed in a dark drawer for 72 h prior to being attached to an IR sample holder consisting of an aluminum sheet with a circular hole in its center. The stearic acid over-layer was applied from a saturated solution of stearic acid in methanol and applied as a single drop by Pasteur pipette to the photocatalyst sample. The samples were then returned to a dark draw for >72 h prior to the initial reading at 0 h. The reason for this was to have a standard starting point for all the samples. FTIR spectra were obtained between 2800 and 3000 cm^{-1} using a Perkin Elmer Spectrum RX1 FTIR spectrometer. Measurements were taken at 24 h intervals with the samples irradiated using the 4 different lighting conditions.

The concentration of the stearic acid on the surface was assessed using IR absorption spectroscopy. Stearic acid absorbs at 2958 cm^{-1} (C–H Stretch CH_3), 2923 cm^{-1} (symmetric C–H stretch CH_2), and 2853 cm^{-1} (asymmetric C–H stretch CH_2). The peaks are then integrated to give an approximate concentration of stearic acid on the surface. 1 A cm^{-1} in the integrated area between 2800 and 3000 cm^{-1} corresponds to approximately 9.7×10^{15} molecules cm^{-2} [51]. The rate of decay can then be measured by the decrease in concentration over time. The data is given in terms of the raw IR data plotted to show the decrease in integrated area.

The light sources were set up in the lids of cardboard boxes and suspended 25 cm above the surface of the samples.

The three lighting conditions were as follows.

I. UV – 8 W UV 254 nm radiation.
II. White light source – 8 W GE lighting 3500 K. This light source is commonly found in UK hospitals and has the emission spectrum shown in Supplementary information Fig. S.1. The intensity of the white light was measured and found to be 5000 lx at a distance of 20 cm from the light source. This can be compared to the brightness recommended by the department of health for different areas in UK healthcare environment. For example an operating theatre should be between 10,000 and 100,000 lx, a pathology lab is 8000 lx and general corridors are up to 100 lx. Also light intensity measurements performed at the UCLH Eastman Dental Hospital have shown that a typical dental chair has a light intensity reading of around 250 lx. Both the UV and visible light sources have been extensively used by us and other groups [23]. An increase in light intensity should result in an increase in photoactivity hence photocatalysts for example in wards or hospitals corridors would work slower than those in the test scenario while those in an operating theatre would work faster.
III. Filtered white light source – in the filtered setup we use the white light source, as before but with a sheet of Optivex™ film as a light filter. This film has been designed for use as a UV shield to preserve works of art and is deposited on a 3 mm thick piece of Borosilicate glass. The filter was positioned 1 cm above the samples and completely filled the box to the edges. The setup was such that there was no chance of any light coming from anywhere and arriving at the samples not having passed through the filter. The filter cuts off all radiation below 400 nm [52]. The UV–visible transmission spectrum of the Optivex™ is shown in Supplementary materials section, Fig. S.2.

2.3. Antimicrobial testing

Prior to antibacterial testing, duplicate samples of the Ag-TiO_2, TiO_2 and blank thin films were housed in a dark drawer for 72 h. *E. coli* ATCC 25922 was stored at −80 °C in BHI broth supplemented with 10% glycerol (Oxoid) and maintained by weekly subculture onto 5% blood agar plates (Oxoid). A single colony was inoculated into 10 ml nutrient broth (Oxoid) and incubated for 18 h at 37 °C, in an orbital shaker set at a speed of 200 rpm. A 1 ml aliquot of the resulting culture was removed, centrifuged at 12,000 rpm for 3 min and the pellet re-suspended in 1 ml fresh phosphate buffered saline. A culture containing a final concentration of approximately 10^7 colony forming units ml^{-1} (cfu ml^{-1}) was achieved by adding 330 μl of the washed bacterial suspension to 10 ml phosphate buffered saline to produce an optical density at 600 nm of 0.05 absorbance units on a spectrophotometer (GE Healthcare).

A 50 μl droplet of *E. coli* was inoculated onto the sample, placed within a moisture chamber to prevent droplet evaporation and exposed to the white light source (hospital lighting conditions) for 6 h (designated L+). As a control, duplicate samples were also prepared, but incubated in a foil-encased moisture chamber to prevent light penetration (designated L−). Bacteria were recovered by sampling the surface with a cotton-tipped swab, before the swab was placed in 1 ml phosphate buffered saline, vortexed and serially diluted tenfold. Duplicate 20 μl aliquots were plated out onto MacConkey agar plates (Oxoid), spread and incubated aerobically at 37 °C for 24 h. The resultant colonies were counted to determine the number of surviving colony forming units per ml. The experiment was performed in duplicate on at least three separate occasions to provide data which could be analyzed statistically, using the Mann–Whitney's *U* test.

All microbiology was carried out against three different substrates, plain glass microscope slides and microscope slides coated in either pure titania or silver loaded titania. Two different controlled lighting environments, i.e. light (white light source) and dark were used. The same type of light source was used in these experiments and was kept at a distance of 20 cm from the samples.

MRSA testing was carried out in exactly the same way but substituting the light resistant strain of MRSA (EMRSA-16) for the *E. coli* bacteria. There are currently two epidemic strains of MRSA infecting UK hospitals, EMRSA-15 and EMRSA-16. Of these two, tests have shown EMRSA-16 to be the most tolerant to light and hence EMRSA-16 was chosen for the experiments.

3. Results and discussion

TiO_2 films were prepared using a sol–gel method by dip-coating glass slides into a sol made from titanium n-butoxide, n-butanol, isopropanol, acetonitrile and water, at room temperature. The films were calcined at 500 °C for 1 h and allowed to cool to room temperature over 12 h. Half of the films were then post-treated by dipping into a methanolic solution that contained silver nitrate. These films were then irradiated for 1 h using 254 nm radiation to generate orange coloured films that had silver nanoparticles bound to the surface [53,54]. Attempts to produce control films containing just the silver nanoparticles on the glass surface failed to produce stable films making it impossible to use these control substrates. The TiO_2 substrate plays an important role in the formation of the nanoparticles which fail to adhere to the glass surface. In this paper the sample names of TiO_2 and Ag-TiO_2 are used to refer to the un-coated and nanoparticulate silver coated films. The films were either stored in a clean, dark drawer for >72 h prior to any testing

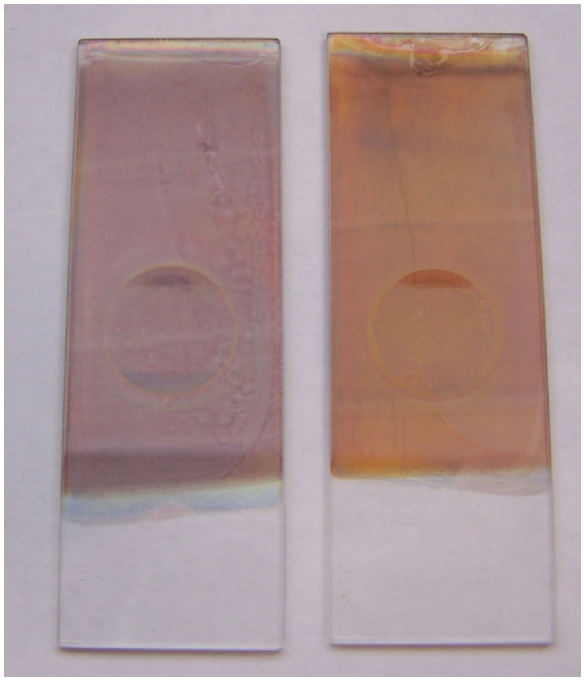

Fig. 1. Photograph showing the difference in colour between sample Ag-TiO_2 (purple on the left) and Ag-TiO_2-UV (orange on the right). Note that the microscope slides contained a 1 cm well cavity ca. 1 mm deep to make them suitable for microbiology testing.

or were irradiated using UV 254 nm radiation to ensure optimum cleanliness of the surface. In the latter case the sample references are TiO_2-UV and Ag-TiO_2-UV respectively.

Both TiO_2 and Ag-TiO_2 films were tested for adherence to the microscope slide substrate using a variety of materials. In all cases the films were resistant to scratching by finger nails, HB pencil, 2H pencil and a steel scalpel but were scratched easily by a diamond tip pencil. Neither of the film sets TiO_2 or Ag-TiO_2 were lifted by the application of Scotch tape. The films were stable when soaked for 2 h in methanol, acetone, distilled water, 2 M HCl but were dissolved in 2 M NaOH.

3.1. Characterization

The TiO_2 films were colourless in appearance and translucent. There was however a slight sheen on the glass making it obvious where the film was on the microscope slide. The Ag-TiO_2 films as made were uniformly orange in colour and transparent (Fig. 1). After storage in dark for >72 h the films were purple in colour (Fig. 1). UV irradiation (10 min, 254 nm, 8 W lamp) or being left under indoor lighting conditions for an extended period (1 h), turned the Ag-TiO_2 films orange while the TiO_2 films were visually unchanged. The orange colour remained indefinitely if left out in the lit room (standard indoor lighting) but slowly returned to purple on placement in the dark over 72 h. This observation indicates that a reversible photo-induced change is occurring leading to the colour change. Colour analysis showed Lab* colours for the two films corresponding to Ag-TiO_2 (purple): $L^* = 79.2$, $a^* = 6.4$ and $b^* = -11.6$ with a dominant wavelength at 444.1 nm and Ag-TiO_2-UV (orange): $L^* = 75.7$, $a^* = 10.3$ and $b^* = -4.8$ and a dominant wavelength at 528.2 nm. The dominant wavelength has been red shifted with the shift from purple to orange in the presence of UV radiation.

It was previously demonstrated that the photochromic effect was due to a change in oxidation state of the silver particles from metallic to silver oxide [53,55]. UV or indeed visible light was seen to induce the metallic state (orange films) while storage in the dark induces the oxide state (purple films). UV-irradiation of TiO_2 is known to excite electrons from the valance band into the conduction band leaving behind an electron hole in the valance band. In pre-dark stored silver doped titania system, the excited electrons then react with oxidized silver species reducing them down to silver atoms [56], changing the colour of the film. The silver oxide nanoparticles were shown to change from less coloured oxide to more coloured metal, displaying photochromism [53,54,56,57]. The silver nanoparticles on the surface of the Ag-TiO_2 films have an enhanced colouration due to a surface plasmon resonance which is a function of the particle size, shape and local refractive index [58,59]. In this case, the irradiated orange surface is in fact the surface containing the silver nanoparticles with the duller purple surface containing the oxidized species. If left in the dark but in the presence of oxygen the silver nanoparticles will revert to the purple colour as they oxidize.

$$\text{Silver oxide (purple)} \overset{h\nu + TiO_2}{\underset{\text{air}}{\rightleftarrows}} \text{Silver (orange)} + \text{Oxygen}$$

This hypothesis was not only verified by evidence from the literature on related TiO_2 with surface embedded silver nanoparticles [57,60] but also backed up by us in an in-house experiment using Schlenk flasks. Purple and orange samples were sealed in separate Schlenk flasks and evacuated. The separate transformation was then attempted in vacuum. The purple sample was irradiated and observed to turn orange and the orange samples were stored in the dark for 72 h and observed to remain orange. This indicates that the backward reaction, silver (orange) to silver oxide (purple) is dependent on oxygen but the forward reaction is only photo-dependent, as shown in the equation above.

AFM was used to observe the particles on the surface of the Ag-TiO_2. Fig. 2 shows the particles of silver oxide that coat the surface without obscuring the entire TiO_2 surface. The range of particle diameters is between 50 and 150 nm. The underlying surface can be seen in the TiO_2 sample with a much lower degree of roughness (Fig. 2b). Surface roughness (Rq) values were: 10.2 nm = Ag-TiO_2 and 1.97 nm = TiO_2. Surface coverage of silver nanoparticles on the titania surface was estimated at 64% from height information in AFM images. Given the median and standard deviation in heights of crystallites observed in the non-coated sample, it was taken that anything larger than the median height plus one standard deviation of this value in the silver nanoparticle sample was given rise to the presence of a silver nanoparticle.

X-ray diffraction of both Ag-TiO_2 and TiO_2 films showed prominent reflections at 25.3, 38.6 and 48.1° 2θ that correspond to the anatase structure of TiO_2. Notably the thin silver oxide surface-layer in Ag-TiO_2 could not be seen by XRD. Raman spectroscopy (Fig. 3) showed the presence of the anatase structure in both TiO_2 and Ag-TiO_2 with no contribution from the rutile phase. Anatase is often observed as the majority phase when TiO_2 is sintered at 500 °C for short periods, in this case 1 h. Rutile becomes dominant at higher temperatures or when TiO_2 is sintered for longer periods and at higher temperatures [7].

Sample Ag-TiO_2 hereon refers to a sample that has been stored in a dark drawer for 72 h and is therefore purple in colour and contains silver oxide on the surface unless specifically stated otherwise.

Scanning electron microscopy (SEM) images of the TiO_2 films shows a clean smooth surface to the film with deep cracks observed frequently throughout. The film is extremely well adhered to the microscope slide substrate but has cracked in places, due to contraction of the dip-coated xerogel during the sintering process. Where they have cracked the break is clean and propagates until a boundary is encountered, Fig. 4. The edges are smooth and regular and the thickness can be estimated to be ca. 200 nm.

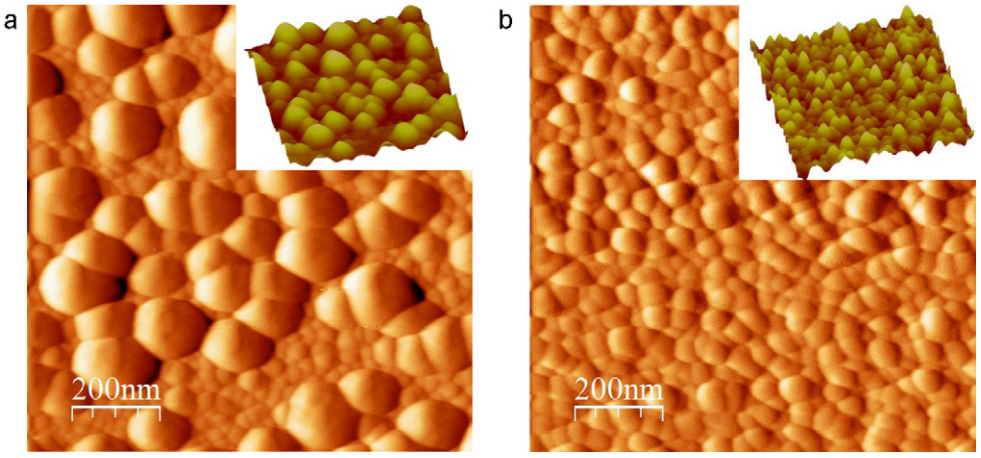

Fig. 2. Two-dimensional AFM images with three dimensional surface inset for; (a) the silver oxide nanoparticles on top of the titania substrate Ag-TiO_2, (b) the uncoated TiO_2.

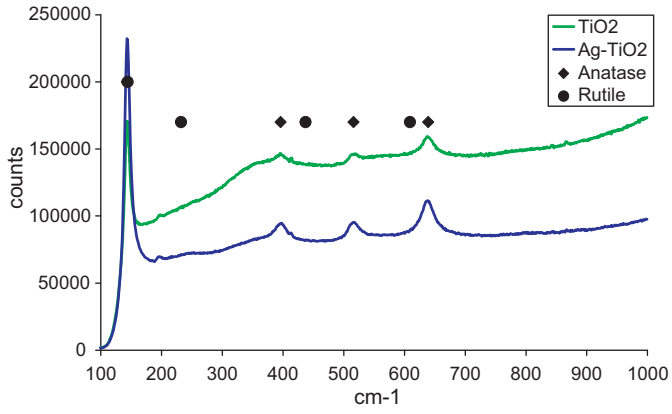

Fig. 3. Raman spectroscopy of samples TiO_2 and Ag-TiO_2 showing the anatase phases of TiO_2.

In the case of Ag-TiO_2 the films appear identical to the TiO_2 but with the addition of nanoparticles on the surface (b). The film thicknesses were seen to be ca. 200 nm from side on SEM and the particles of Ag_2O are evenly spread over the entire surface with higher concentrations in and around the cracks. EDX shows a 1:2 elemental ratio of Ti:O for both samples with the particles on the surface of Ag-TiO_2 showing silver content. The silver content was close to the resolution of the machine at around 0.5 at.% however the results show that there is silver doped into the layer of TiO_2 to <0.5 at.% indicating that doping has been achieved.

XPS analysis showed the presence of silver, oxygen and titanium in both Ag-TiO_2 and UV-Ag-TiO_2 samples. The silver 3d 5/2 peak was noted at 368.0 eV with a shift of 0.3 eV between the two samples Ag-TiO_2 and UV-Ag-TiO_2. This was however, not significantly above the error associated with the measurements so as to be significant in determining the difference between silver states on the different samples. The XPS shifts in silver are significantly close together to hinder determination of the different oxidation states [57]. Observation of the silver oxidation state by XPS without exciting the TiO_2 to form the silver proved unobtainable. Peak area calculations from the XPS show that the silver is present, ~6.3 at.% at the surface. XPS analysis is complicated in this system as the incident X-rays seem to promote the oxide to elemental silver on the surface that is under analysis yielding false positive readings for silver rather than silver oxide. X-Ray radiation promotes the change from purple to orange making it very difficult to observe the purple phase using this technique with long scans. Many of the scans showed the presence of silver metal regardless of storage in the dark. The instability of the films is shown in Supplementary material, Fig. S.3. where a shift in Auger electron position is noted to lower energy, i.e. oxide to elemental silver during the course of the experiment.

UV–visible–IR spectroscopy was carried out using the same films prepared on both glass and quartz substrates. Quartz has a better observation window in the UV–visible region and enabled a better measurement of the band onset using a Tauc plot without the interference of the underlying glass band. The UV–visible–NIR spectroscopy Transmission results are given in Fig. 5 and show that samples TiO_2 and Ag-TiO_2 are almost the same with a small decrease in transmission due to the silver ions on the surface and a minimal red shift in the position of the absorption when comparing Ag-TiO_2 to TiO_2. The features in the visible region are due to reflection effects rather than absorption and allow us to calculate

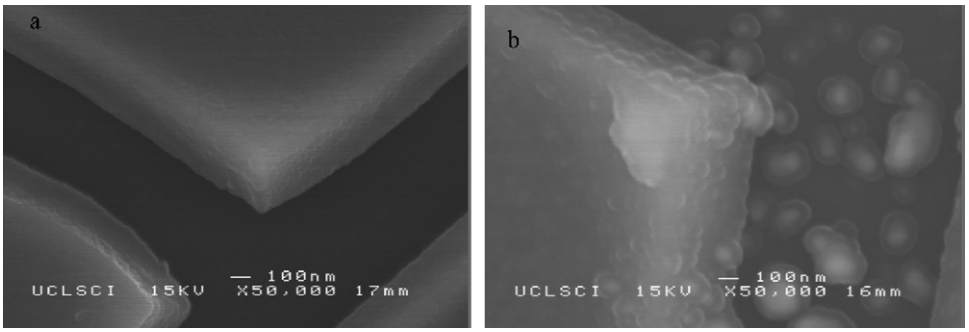

Fig. 4. SEM electron micrographs of (a) TiO_2 and (b) Ag-TiO_2. Both images show the plate like structure to the films and the presence of particles on the silver enhanced samples.

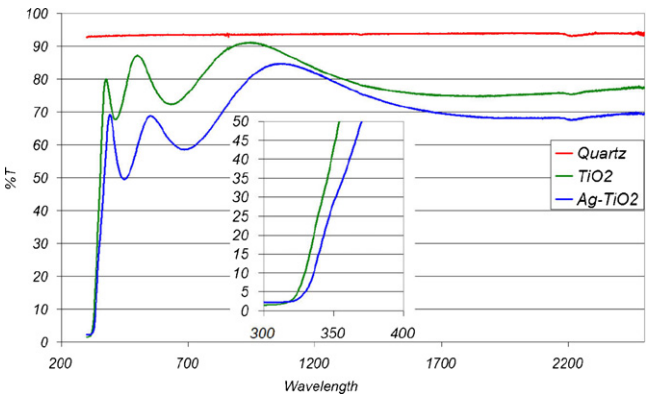

Fig. 5. Results for the UV–visible–IR spectrometry using quartz slides. Inset is a close up of the shift in absorption band onset for the different samples.

the thickness of the film coating using the Swanepoel method [61]. Quartz is seen to have no features above 190 nm.

With use of the Swanepoel method [61] the thickness of the films from reflectance data were estimated to be 196 nm in the case of TiO_2 and 211 nm in the case of Ag-TiO_2, indicating that the silver has very little effect on the film thickness with both being in the region of 200 nm as measured by side on SEM.

Tauc plots, were used to estimate the band onset from the UV–visible–IR absorption data for the two samples deposited on quartz. A Tauc plot is a plot of $(a \times h\nu)^{1/2}$ against energy where "a" is the absorbance of the material [62,63]. Tauc plots are recognized as a reliable method of estimating the band onset for these types of materials. The data shows a minimal shift in band onset towards the lower energy radiation with the incorporation of silver on the surface of the TiO_2 substrates (3.2 eV for TiO_2 to 2.8 eV for silver coated Ag-TiO_2). In the absence of particle size modification this change in band onset suggests the presence of silver doping into the TiO_2 structure, and ties with the 0.5 at.% seen by EDX in the sample bulk. The function of the silver is to promote the electron transfer from the valance band to the conduction band within the TiO_2 [31]. Band onsets of as low as 2.6 eV have been reported from the doping of TiO_2 with silver [31]. It is also likely that the silver oxide present has an effect of mixing the band onsets, adding a feature to the curve in the vertical region. This is seen in the blue line in the inset of Fig. 5. AgO has an optical band onset ~1 eV [64] and Ag_2O has a band gap ~1.45 eV [65] in both cases the band gap is dependent of particle and film size and morphology.

3.2. Functional testing

The films were tested for their functional properties using water contact angle measurements and the photo-oxidation of stearic acid under three different lighting conditions.

Water contact angle measurements were taken both on a pre-irradiated film (UVC – 254 nm, 30 min) and on a film that had been stored in the dark for >72 h. The superhydrophilicity arises as a result of the production of a hydroxylated surface [66]. 254 nm UV-light was used to pre-clean and activate all the films after the initial water contact angle measurement to ensure that the films were clean and that the surface was fully hydroxylated (Table 1).

The exposure to UV light had no effect on the glass microscope slides that were used as the substrate however it did have a pronounced effect on the water contact angle of both the functional thin films. The microscope slide had a comparatively low water contact angle. Glass would be typically expected to have a water contact angle of about 70°, the low water contact angle of the microscope slide indicated that the surface was very clean [66]. These slides were pre-cleaned and medically sterile as supplied. TiO_2 became superhydrophilic with a water contact angle changing from 64° to 8°. TiO_2 would be expected to have a significant water contact angle reduction upon irradiation leading to super hydrophilic properties [1,2,67]. In the case of the silver enhanced films, the hydrophilicity is markedly changed in much the same way as noted for TiO_2. The nanoparticles on the surface contribute to surface roughness which should enhance either the superhydrophilic or hydrophobic properties [68,69] though this effect seems to have been insignificant. No significant difference in the surface wetting properties occurred after silver loading; even though a 64% surface coverage was observed.

Table 1
Results from the water contact angle measurements: "UV" indicates that the surface has been irradiated under 254 nm for 30 min prior to the measurements taking place. All measurements are accurate to ±2°.

Sample name	Water contact angle
Microscope slide	25 (2)°
Microscope slide – UV	24 (2)°
TiO_2	64 (2)°
TiO_2-UV	8 (2)°
Ag-TiO_2	60 (2)°
Ag-TiO_2-UV	8 (2)°

It is important to note from the earlier observations that there is likely a significant difference in the surface of the silver enhanced samples, i.e. Ag-TiO_2 has silver oxide particles while Ag-TiO_2-UV has silver nanoparticles. It does appear however that the presence of either of the nanoparticles has no effect on the hydrophilicity. When irradiated with visible light using the Optivex™ filter, the water contact angle measurements of the Ag-TiO_2 samples gave a water contact angle of 8°, while the TiO_2 films irradiated under the same conditions remained at 60°. This demonstrated that the Ag-TiO_2 becomes superhydrophilic with visible light irradiation while using the TiO_2 film did not. This is to the best of our belief, the first example of unambiguous visible light induced superhydrophilicity in thin films.

The photoactivity of the films was quantified using the photo-oxidation of stearic acid under three different lighting conditions, a 254 nm UV light source, a white light source commonly found in UK hospitals [70] and the same light source with a UV filter to absorb any stray high energy photons. Figs. S.4, S.5 and 6 show the decreasing concentration of stearic acid on the surface of the three different samples over time using three different irradiation sources. The raw data shown in the supplementary material is summarised in Table 2, and shows that different photoactivity is observed for the different samples under the different lighting conditions.

In all cases there was no appreciable change in concentration of stearic acid observed on the blank microscope slides during the irradiation. In contrast TiO_2 and Ag-TiO_2 both show significant destruction with almost all the stearic acid photo-oxidized within 24 h when using UVC (254 nm) light. Mills and Wang has shown that a reliable quantification for the stearic acid decrease over time can be calculated from the integrated area of the IR spectrum [51]. 1 unit of integration between 2700 and 3000 $cm^{-1} \approx 9.7 \times 10^{15}$ molecules cm^{-2} [51]. This equates to give a rate of $\sim 1.1 \times 10^{14}$ molecules cm^{-2} h^{-1} for both TiO_2 and Ag-TiO_2; with equivalent rates observed within the accuracy of the experiment. Under UV conditions the silver neither improved not worsened the self-cleaning photoactivity of the TiO_2. Using a white light source commonly found in UK healthcare environments [70] (GE lighting 2D fluorescent GR10q-835 white, 28 W), TiO_2 shows a minimal reduction while Ag-TiO_2 however showed a significant reduction in stearic acid concentration. Using the conversion outlined by Mills and Wang [51] rates of destruction of $\sim 1.6 \times 10^{14}$ and $\sim 4.2 \times 10^{14}$ molecules cm^{-2} h^{-1} again for samples TiO_2 and Ag-TiO_2 respectively were observed. N-doped TiO_2 sam-

Table 2
The number of molecules of stearic acid photo-oxidized during the irradiation by the different light sources. Rates are given as molecules cm^{-2} h^{-1}.

	UV-254 nm – 29 h		White light – 96 h		White light with Optivex™ filter – 500 h	
	Molecules oxidized	Rate	Molecules oxidized	Rate	Molecules oxidized	Rate
TiO_2	3.32×10^{16}	1.14×10^{15}	1.49×10^{16}	1.55×10^{14}	1.49×10^{14}	2.99×10^{11}
Ag-TiO_2	3.30×10^{16}	1.14×10^{15}	4.05×10^{16}	4.22×10^{14}	3.12×10^{16}	6.25×10^{13}

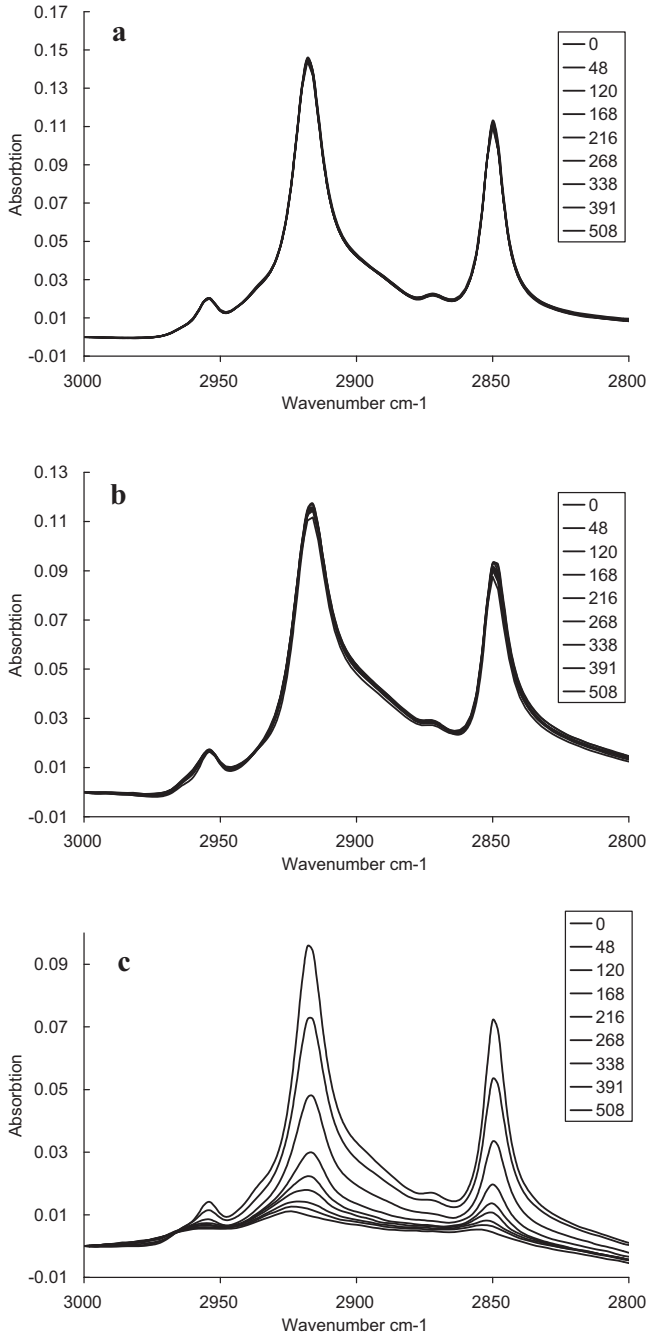

Fig. 6. Raw data showing the photo-oxidation of stearic acid molecules on the surface of the three samples over 500 h using a white light source typically found in UK hospitals and a sheet of Optivex™ coated glass. This is to our knowledge the first unequivocal evidence of visible light photocatalytic destruction of Stearic acid. Lines times are in order of height. The three samples are: (a) blank microscope slide; (b) pure titania; (c) silver enhanced titania. In all cases, the area under the curve indicates the amount of stearic acid on the surface and the heights of the lines represent time with the highest peaks corresponding to the shortest irradiation time.

ples prepared by APCVD were previously seen to show a destruction of $\sim 1.4 \times 10^{14}$ molecules cm^{-2} h^{-1} [24,25]. S-doped samples again prepared by APCVD [23,24] were shown to have comparable rates of destruction with $\sim 1.8 \times 10^{16}$ molecules cm^{-2} destroyed in 168 h and a corresponding rate of $\sim 1.1 \times 10^{14}$ molecules cm^{-2} h^{-1} again using the same lighting conditions. The silver enhanced TiO_2 sample Ag-TiO_2 is therefore >3 times more efficient than both the N-doped TiO_2 and S-doped TiO_2 samples prepared by APCVD analogously tested under hospital lighting conditions. The silver coated samples are found to significantly outperform the pure titania by more than a factor of two, using visible light, but when under UV lighting the rates were comparable. This implies that surface silver doping does not induce as much electron hole re-combination of photoelectron–hole pairs as observed in N and S doped titania [71]. These rates are noted as being less than that observed for the UV irradiation but are however significantly high as rates of stearic acid photo-degradation under white light conditions.

With a band onset of 3.2 eV the anatase sample, TiO_2, should show no activity in the absence of UV light (<385 nm) indicating that there may be a small amount of higher energy photons released from the 2D fluorescent bulb light source. The emission spectrum for the bulb, Fig. S.1 shows no emission below 410 nm however the spectral data was only supplied down to 380 nm [70]. It has been noticed in the past that older the white light sources can give good performance for white light photocatalysis which is believed to be due to the handling of the white light sources. As the bulbs are handled the phosphor coating on the inside of the fluorescent tube can become unstuck from the surface allowing for the leaking of a very small fraction of higher energy radiation to escape. This would increase the UV component and give the appearance of better white light photocatalysis; a "False Positive Result".

To counter this, the experiment was run with a piece of Optivex™ glass placed in between the sample and the same light source as used above. Optivex™ glass is commonly used to preserve precious artwork from the damage caused by UV light and absorbs virtually all radiation below 400 nm. The UV–Vis spectrum for a sample of Optivex™ coated glass is shown in Supplementary material Fig. S.2 clearly indicating that at wavelengths below 400 nm there is almost no transmission.

The photo-oxidation of stearic acid using filtered white light on the TiO_2 and Ag-TiO_2 films is now seriously impeded as shown in Fig. 6. Sample TiO_2 has negligible degradation, indicating that white light results shown in Fig. S.5 are due to stray high energy photons $\lambda < 400$ nm in wavelength, and highlighting the validity of using the filter for true visible light photocatalytic observations. Under these conditions, $\lambda > 400$, sample Ag-TiO_2 retains activity and is 200× as effective at destroying stearic acid than the control TiO_2, Table 2. These films are therefore clearly active with incident radiation of wavelength above 400 nm. The activity is lower than that observed under the unshielded white light source which is due to a combination of the loss in intensity of visible light from the ~80% transmission through the Optivex™ glass and due the loss of the UV part of the spectrum as measured by UV–Vis transmission spectra and confirmed by lux readings at 20 cm from the light source (16,000 lx vs. 13,000 lx).

The results now conclusively suggest that the sample Ag-TiO_2 is indeed displaying visible light driven photo-oxidation of stearic acid using the sample TiO_2 as a control to account for any stray

photons of higher energy. To our knowledge this is the first unambiguous display of visible light photocatalysis.

Table 2 clearly shows that there is significant photo-chemical activity associated with samples TiO_2 and Ag-TiO_2 under both UV and white lighting conditions. Under UV irradiation both photocatalysts performed the same with a highly significant improvement on the blank slide. In contrast, when the incident light energy was restricted, i.e. a light source that contained visible light with no UV-component, the silver coated samples become far more effective than the pure titania showing photo-activity with more than two hundred times the oxidizing potential of the surface during the 96 h experiment when compared to the pure TiO_2 sample. In both cases there were significant reductions in photo-activity between the UV and the white light source, which is to be expected given the differences in the intensity outputs for the two sources. Under hospital lighting conditions there will likely be an equilibrium between the silver nanoparticles on the surface of the titanium, and the silver oxide in sample Ag-TiO_2. Oxidation reactions will be occurring at the same time as photo-reduction of the silver oxide by the TiO_2. The reactive oxygen species in the photo-reduction will then be free to take part in the photo-oxidation of the stearic acid. However pure TiO_2 would not be as significantly photo-activated by the light source, as very little of the radiation will be below the 385 nm threshold that is required to excite an electron from the valance band into the conduction band of TiO_2. Therefore a reduction in activity under the white light conditions should be observed. This is clearly not happening, indicating that the surface silver is interacting with the TiO_2 and allowing it to absorb lower energy light more efficiently than TiO_2 on its own. This could be in the form of a coupling between the plasmon resonance from the silver nanoparticles and the band structure of the TiO_2. It might therefore be possible to enhance the properties of a photocatalyst by tuning the particle size of the silver applied to its surface. The surface plasmon resonance effect (controlled by the particle size) could couple to the photocatalyst's intrinsic band onset properties and lead to enhanced photocatalysis at low energy. This is similar to that observed when the plasmon resonance of gold particles couples to the absorption of a dye leading to dye-sensitized enhanced properties [72].

In the case of the UV irradiation the TiO_2 is saturated with UV light so no change in activity would be expected from the addition of the silver nanoparticles to the surface. All light photons will be higher in energy than both the band onset and the light needed to excite the surface plasmon effects hence no enhancement is observed due to the presence of silver on the surface.

3.3. Microbiological testing

The samples were tested for their inherent antimicrobial effects using both *E. coli* and an epidemic strain of MRSA, EMRSA-16. Both of these organisms represent significant problems for western healthcare environments and the control of their reproduction is seen as key to tackling the issues of infection rates within our hospitals [20]. Fig. 7 shows the results from experiments using EMRSA-16, a light tolerant strain of MRSA after 12 h incubation in the presence of white light. A significantly enhanced kill is present only with the results representing the experimental conditions of light and the silver active surface (Ag^+/L^+). This is indicative of the silver particles enhancing the light activated surface's photocatalytic properties and the TiO_2 enhancing the silvers toxic properties, evidence of a synergistic relationship between the two destructive routes. Ag-TiO_2 without the light (Ag^+L^-) and TiO_2 (Ag^-L^-) on its own (Ag^-L^-/Ag^-L^+) show negligible kill. The EMRSA-16 strain used is light tolerant, and appears unaffected by the silver ions in the dark. MRSA is known to be highly susceptible to destruction from light activated antimicrobial surfaces so is not resistant to photocatalytically produced radicals from the TiO_2. It is therefore possible to conclude that the photoinduced destruction is due to radical production in the TiO_2 from the white light photocatalytic effects induced by the silver. These radicals however require the silver to be present as they are formed from white light. The fact that the TiO_2 on its own shows negligible kill in the presence of white light indicates that firstly our white light source has negligible quantities of UV light and secondly that the photoactivity observed in the more active sample is due to an enhanced photocatalytic effect. It is however possible that the TiO_2 with the silver is promoting the photo-assisted release of silver ions which in turn are killing the bacteria. It is not easy to determine if the kill is due to the direct photodegradation, i.e. radical production, or if photoassisted silver ion release kills the organism. EMRSA-16 was found to be more tolerant to light than the EMRSA-15 strain and similar if not enhanced results, i.e. greater kills in all light experiments, would be expected in identical experiments using EMRSA-15.

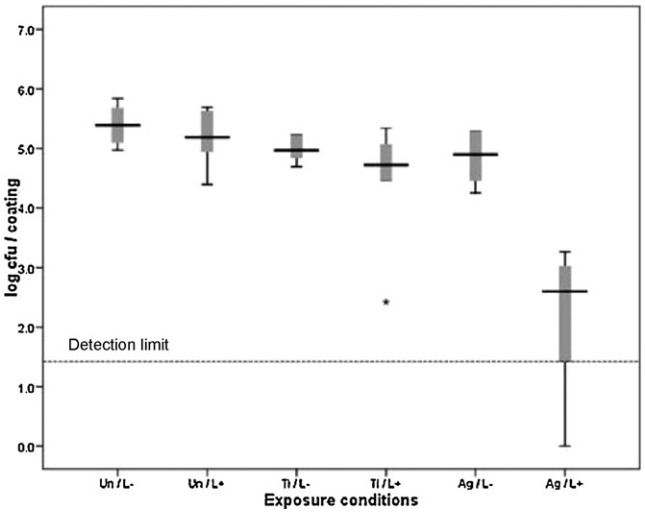

Fig. 7. Microbiology data (EMRSA-16) showing the three different samples under the 2 different conditions of testing, light on (L+, hospital lighting conditions) and light off (L−) for 12 h using. The first 2 data sets are from blank microscope slides, Un, the next 2 data sets are the pure titania, TiO_2 and the final 2 data sets are from sample Ag-TiO_2. Median values are displayed in colony forming units present on the test slides after 12 h of incubation at room temperature and are represented by the thick horizontal line. The base and top of each box represents the 25% and 75% quartiles respectively, and the error bars, the 10% and 90% percentiles. The detection limit of the assay is also shown.

Experiments using *E. coli*, a microbe that is reputed as being one of the hardest to destroy using light activated surfaces was easily dispatched using these surfaces. Both silver containing conditions resulted in a total kill within 6 h of the 12 h experiment, hence the data presented in Fig. 8 is for 6 h rather than 12 h. A 99.996% (4.4 $\log_{10}$ cfu/coating) decrease in the number of viable bacteria was observed on the Ag-TiO_2 films incubated under white light for 6 h, compared with the TiO_2 films incubated under the same light conditions for the same time period. This shows that there is a significant enhancement in the killing of *E. coli* ($p < 0.001$) due to the presence of the silver ions when comparing Ag-TiO_2 and TiO_2 under white light conditions. A similar decrease in the bacterial number was demonstrated when the viable counts from Ag-TiO_2 incubated in the absence of light were compared with the viable counts from TiO_2 incubated in the absence of light, indicating that the observed effect was independent of white light exposure. This is highly indicative of high toxicity of the silver ions, rather than a light induced effect.

No significant difference in bacterial numbers was observed on the TiO_2 thin films incubated in the dark compared with those exposed to white light for 6 h, indicating that the white light did not activate the TiO_2 thin films as the white light source contained

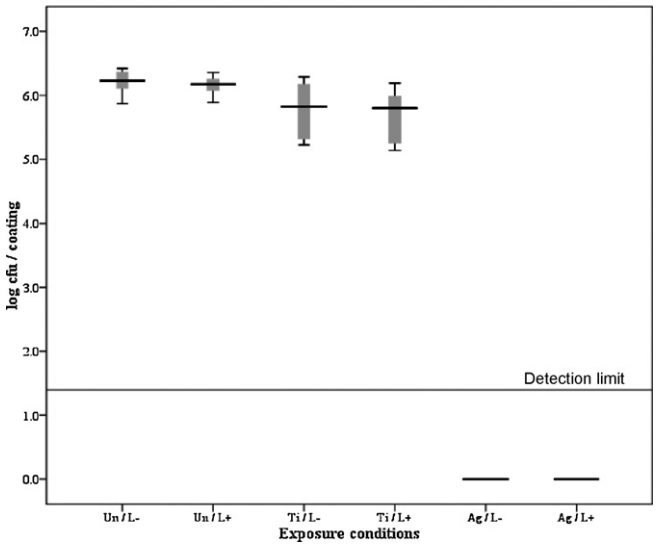

Fig. 8. Microbiology data showing the three different samples under the 2 different conditions of testing, light on (L+, hospital lighting conditions) and light off (L−) for 6 h. The first 2 data sets are from blank microscope slides, Un, the next 2 data sets are sample TiO_2 and the final 2 data sets are from sample Ag-TiO_2.

no UV component. Additionally, no significant decrease in bacterial count was observed on the blank microscope slides exposed to white light (when compared to those incubated in the absence of white light), demonstrating that the white light did not have an inhibitory effect on the viability of *E. coli*. All other conditions resulted in negligible kill.

These results indicate that *E. coli* is killed effectively by the silver as comparable data were seen in both Ag^+L^+ and Ag^+L^- samples (i.e. the sample Ag-TiO_2 kills *E. coli* in both the light and the dark), whereas for EMRSA-16 the kill was significantly enhanced by the light.

4. Conclusions

The addition of surface bound silver/silver oxide nanoparticles has been shown to significantly enhance the activity of a TiO_2 photocatalyst, for a number of its functional properties. Structurally the samples were found to be the anatase structure of TiO_2 with surface bound silver containing nanoparticles. The silver was observed as either silver oxide or pure silver depending on the state of the underlying TiO_2 film. Storage in the dark but in air led to partial oxidation of silver to silver oxide nanoparticles while irradiation under UV light reduced the silver oxide to silver on the surface. These thin films display photochromic behaviour as a colour change between purple, oxide and orange, silver metal.

The silver nanoparticles caused a shift in the band onset allowing the harvesting of lower energy photons and the occurrence of white light induced photocatalysis. This was attributed to an interaction between the surface plasmon resonance effects of the silver nanoparticles and the band properties of the TiO_2 leading to enhanced photocatalysis under conditions where the quantity of UV-light is significantly reduced, such as those found indoors.

It has been possible to show the presence of visible light photocatalysis using a light source commonly found in UK hospitals and a piece of Optivex™ glass as a UV filter. A TiO_2 photocatalyst was used as a control to detect the presence of any UV passing through the filter. Any UV-radiation incident on the samples would have led to some form of photoactivity on the TiO_2 sample over the time scale leading to a difference in the raw data traces between the TiO_2 and the blank samples. The fact that the stearic acid photo-oxidation results for these two samples are the same in appearance means that there is no leakage of UV-light in the light source and setup. The presence of photocatalysis from the silver enhanced samples under these conditions can therefore reliably be considered to be due to light of energy within the visible spectrum ($\lambda > 400$ nm). These silver containing films prepared by sol–gel synthesis exhibit the up to 4 times the rate of photo-oxidation of stearic acid under white lighting conditions compared to those seen from APCVD synthesis of N-doped and S-doped TiO_2 reported previously [23–25,43].

The Ag-TiO_2 films have proved to be exceptional visible light photocatalysts under visible light, even in the presence of a UV filter. This is the first example of unambiguous visible light photocatalysis and photo-induced super hydrophilicity along side a TiO_2 control that shows no activation.

The silver enhanced samples show real promise in the field of self-cleaning coatings and could have significant applications in US and UK healthcare environments. The silver enhanced samples, Ag-TiO_2 showed a 4.4 $\log_{10}$ kill or indeed (99.996% reduction) of *E. coli* bacteria during the 6 h of the experiment making these samples highly efficient as antimicrobial agents. In the presence of light the Ag-TiO_2 samples showed a 3.5 log kill with a light resistant strain of MRSA. It is however likely that the killing effect on *E. coli* is hugely enhanced as a result of the presence of the silver rather than purely the TiO_2. The MRSA as shown in Fig. 7 is killed due to the light activated surface, most probably enhanced by the presence of the silver nanoparticles.

This double pronged approach involving a photocatalyst and silver is beneficial over just the photocatalyst and indeed just the silver as the photocatalytic surface adds a degree of adherence to the substrate allowing the silver ions to bond better to the surface. The enhancement of silver activation allows less silver to be used which will have cost implications given the high cost of precious metals. The synergistic effect allows more bacteria to be killed in a shorter time period and allows for the multi-directional mechanism of action making these a more potent killer of all bacteria types. This is important as different bacteria have different susceptibility to the different anti-microbial approaches. MRSA for instance is relatively easily deactivated using light activated anti-microbial surfaces but is more resistant to silver ions. Conversely *E. coli* is hard to deactivate using a light activated anti-microbial agent but is highly susceptible to silver ions. The duel approach therefore provides a multi-functional surface that is effective against more types of bacteria and therefore more effective across the board.

Acknowledgements

The authors would like to acknowledge Emily Smith and the EPSRC for performing the XPS analysis at the University of Nottingham. IPP thanks the RSC Wolfson Trust for a merit award.

Appendix A. Supplementary data

Supplementary data associated with this article can be found, in the online version, at doi:10.1016/j.jphotochem.2011.04.001.

References

[1] A. Mills, S. Le Hunte, An overview of semiconductor photocatalysis, J. Photochem. Photobiol. A: Chem. 108 (1997) 1–35.
[2] I.P. Parkin, R.G. Palgrave, Self-cleaning coatings, J. Mater. Chem. 15 (2005) 1689–1695.
[3] T.L. Thompson, J.T. Yates, Surface science studies of the photoactivation of TiO_2-new photochemical processes, Chem. Rev. 106 (2006) 4428–4453.
[4] P. Evans, M.E. Pemble, D.W. Sheel, Precursor-directed control of crystalline type in atmospheric pressure CVD growth of TiO_2 on stainless steel, Chem. Mater. 18 (2006) 5750–5755.

[5] A. Mills, N. Elliott, I.P. Parkin, S. O'Neill, R.J.H. Clark, Novel TiO_2 CVD films for semiconductor photocatalysis, J. Photochem. Photobiol. A: Chem. 151 (2002) 171–179.
[6] A. Kafizas, S. Kellici, J.A. Darr, I.P. Parkin, Titanium dioxide and composite metal/metal oxide titania thin films on glass: a comparative study of photocatalytic activity, J. Photochem. Photobiol. A: Chem. 204 (2009) 183–190.
[7] G. Hyett, M. Green, I.P. Parkin, X-ray diffraction area mapping of preferred orientation and phase change in TiO_2 thin films deposited by chemical vapour deposition, J. Am. Chem. Soc. 128 (2006) 12147–12155.
[8] Last accessed http://www.pilkington.com/applications/products2006/english/downloads/byproduct/selfcleaning/default.htm.
[9] A. Kudo, Y. Miseki, Heterogeneous photocatalyst materials for water splitting, Chem. Soc. Rev. 38 (2009) 253–278.
[10] M. Ni, M.K.H. Leung, D.Y.C. Leung, K. Sumathy, A review and recent developments in photocatalytic water-splitting using TiO_2 for hydrogen production, Renew. Sustain. Energy Rev. 11 (2007) 401–425.
[11] D. Leung, X. Fu, C. Wang, M. Ni, M. Leung, X. Wang, Hydrogen production over titania-based photocatalysts, ChemSusChem 3 (2010) 681–694.
[12] W. Curdt, P. Brekke, U. Feldman, K. Wilhelm, B.N. Dwivedi, U. Schuhle, P. Lemaire, Solar and Galactic Composition, vol. 598, 2001, p. 45.
[13] Centre for Disease Control and Prevention. http://www.cdc.gov/ncidod/dhqp/healthDis.html.
[14] R.M. Klevens, J.R. Edwards, C.L.J. Richards, T.C. Horan, R.P. Gaynes, D.A. Pollock, D.M. Cardo, Estimating health care-associated infections and deaths in U.S. hospitals, 2002, Public Health Rep. 122 (2) (2007) 160–166.
[15] Centre for Disease Control and Prevention. http://www.cdc.gov/ncidod/dhqp/hai.html.
[16] R. Douglas-Scot, The Direct Medical Costs of Healthcare-Associated Infections in U.S. Hospitals and the Benefits of Prevention, Centers for Disease Control and Prevention, Division of Healthcare Quality Promotion, National Center for Preparedness D, and Control of Infectious Diseases, Coordinating Center for Infectious Diseases, 2009.
[17] Office for national statistics. Last accessed from: http://www.statistics.gov.uk/pdfdir/cdif0809.pdf.
[18] Department of Health, Winning ways: working together to reduce Healthcare Associated Infection in England, 2003.
[19] D. Mitoraj, A. Janczyk, M. Strus, H. Kisch, G. Stochel, P.B. Heczko, W. Macyk, Visible light inactivation of bacteria and fungi by modified titanium dioxide, Photochem. Photobiol. Sci. 6 (2007) 642–648.
[20] S. Noimark, C.W. Dunnill, M. Wilson, I.P. Parkin, The role of surfaces in catheter-associated infections, Chem. Soc. Rev. 38 (2009) 3435–3448.
[21] K. Page, M. Wilson, I.P. Parkin, Antimicrobial surfaces and their potential in reducing the role of the inanimate environment in the incidence of hospital-acquired infections, J. Mater. Chem. 19 (2009) 3819–3831.
[22] M.-S. Wong, W.-C. Chu, D.-S. Sun, H.-S. Huang, J.-H. Chen, P.-J. Tsai, N.-T. Lin, M.-S. Yu, S.-F. Hsu, S.-L. Wang, H.-H. Chang, Visible-light-induced bactericidal activity of a nitrogen-doped titanium photocatalyst against human pathogens, Appl. Environ. Microbiol. 72 (2006) 6111–6116.
[23] C.W. Dunnill, Z.A. Aiken, A. Kafizas, J. Pratten, M. Wilson, D.J. Morgan, I.P. Parkin, White light induced photocatalytic activity of sulfur-doped TiO_2 thin films and their potential for antibacterial application, J. Mater. Chem. 19 (2009) 8747–8754.
[24] C.W. Dunnill, I.P. Parkin, N-doped titania thin films prepared by atmospheric pressure CVD using t-butylamine as the nitrogen source: enhanced photocatalytic activity under visible light, Chem. Vap. Deposition 15 (2009) 171–174.
[25] C.W. Dunnill, Z.A. Aiken, J. Pratten, M. Wilson, D.J. Morgan, I.P. Parkin, Enhanced photocatalytic activity under visible light in N-doped TiO_2 thin films produced by APCVD preparations using t-butylamine as a nitrogen source and their potential for antibacterial films, J. Photochem. Photobiol. A: Chem. 207 (2009) 244–253.
[26] A. Kafizas, C.W. Dunnill, I.P. Parkin, Combinatorial atmospheric pressure chemical vapour deposition (cAPCVD) of niobium doped anatase; effect of niobium on the conductivity and photocatalytic activity, J. Mater. Chem. 20 (2010) 8336–8349.
[27] M.E.A. Warwick, C.W. Dunnill, R. Binions, Multifunctional nanocomposite thin films by aerosol-assisted CVD, Chem. Vap. Deposition 16 (2010) 220–224.
[28] A. Zielinska, E. Kowalska, J.W. Sobczak, I. Lacka, M. Gazda, B. Ohtani, J. Hupka, A. Zaleska, Silver-doped TiO_2 prepared by microemulsion method: Surface properties, bio- and photoactivity, Sep. Purif. Technol. 72 (2010) 309–318.
[29] J. Yu, J. Xiong, B. Cheng, S. Liu, Fabrication and characterization of Ag-TiO_2 multiphase nanocomposite thin films with enhanced photocatalytic activity, Appl. Catal. B: Environ. 60 (2005) 211–221.
[30] M.R. Elahifard, S. Rahimnejad, S. Haghighi, M.R. Gholami, Apatite-coated Ag/AgBr/TiO_2 visible-light photocatalyst for destruction of bacteria, J. Am. Chem. Soc. 129 (2007) 9552–9553.
[31] I. Medina-Ramirez, Z. Luo, S. Bashir, R. Mernaugh, J.L. Liu, Facile design and nanostructural evaluation of silver-modified titania used as disinfectant, Dalton Trans. 40 (2011) 1047–1054.
[32] A. Guillén-Santiago, S.A. Mayén, G. Torres-Delgado, R. Castanedo-Pérez, A. Maldonado, I.L. Md Olvera, Photocatalytic degradation of methylene blue using undoped and Ag-doped TiO_2 thin films deposited by a sol–gel process: effect of the ageing time of the starting solution and the film thickness, Mater. Sci. Eng. B 174 (2010) 84–87.
[33] A.V. Emeline, V.N. Kuznetsov, V.K. Rybchuk, N. Serpone, Visible-light-active titania photocatalysts: the case of N-doped TiO(2)s-properties and some fundamental issues, Int. J. Photoenergy 2008 (2008) 258394.
[34] C. Hsyi-En, L. Wen-Jen, H. Ching-Ming, H. Ming-Hsiung, H. Chien-Lung, Visible light activity of nitrogen-doped TiO[sub 2] thin films grown by atomic layer deposition, Electrochem. Solid-State Lett. 11 (2008) D81–D84.
[35] M. Masahiko, W. Teruyoshi, Visible light photocatalysis of nitrogen-doped titanium oxide films prepared by plasma-enhanced chemical vapor deposition, J. Electrochem. Soc. 153 (2006) C186–C189.
[36] F. Peng, L. Cai, H. Yu, H. Wang, J. Yang, Synthesis and characterization of substitutional and interstitial nitrogen-doped titanium dioxides with visible light photocatalytic activity, J. Solid State Chem. 181 (2008) 130–136.
[37] D. Li, H. Haneda, S. Hishita, N. Ohashi, Visible-light-driven nitrogen-doped TiO_2 photocatalysts: effect of nitrogen precursors on their photocatalysis for decomposition of gas-phase organic pollutants, Mater. Sci. Eng. B 117 (2005) 67–75.
[38] A. Borras, C. Lopez, V. Rico, F. Gracia, A.R. Gonzalez-Elipe, E. Richter, G. Battiston, R. Gerbasi, N. McSporran, G. Sauthier, E. Gyorgy, A. Figueras, Effect of visible and UV illumination on the water contact angle of TiO_2 thin films with incorporated nitrogen, J. Phys. Chem. C 111 (2007) 1801–1808.
[39] Z.A. Aiken, G. Hyett, C.W. Dunnill, M. Wilson, J. Pratten, I.P. Parkin, Antimicrobial activity in thin films of pseudobrookite-structured titanium oxynitride under UV irradiation observed for *Escherichia coli*, Chem. Vap. Deposition 16 (2010) 19–22.
[40] Y. Wang, J. Li, P. Peng, T. Lu, L. Wang, Preparation of S-TiO_2 photocatalyst and photodegradation of L-acid under visible light, Appl. Surf. Sci. 254 (2008) 5276–5280.
[41] T. Ohno, T. Mitsui, M. Matsumura, Photocatalytic activity of S-doped TiO_2 photocatalyst under visible light, Chem. Lett. 32 (2003) 364–365.
[42] M. Hamadanian, A. Reisi-Vanani, A. Majedi, Preparation and characterization of S-doped TiO_2 nanoparticles, effect of calcination temperature and evaluation of photocatalytic activity, Mater. Chem. Phys. 116 (2009) 376–382.
[43] C.W Dunnill, Z.A. Aiken, J. Pratten, M. Wilson, I.P. Parkin, Sulfur- and nitrogen-doped titania biomaterials via APCVD, Chem. Vap. Deposition 16 (2010) 50–54.
[44] C.W. Dunnill, I.P. Parkin, Nitrogen-doped TiO_2 thin films: photocatalytic applications for healthcare environments, Dalton Trans. 40 (2011) 1635–1640.
[45] B.K. Sunkara, R.D.K. Misra, Enhanced antibactericidal function of W4+-doped titania-coated nickel ferrite composite nanoparticles: a biomaterial system, Acta Biomater. 4 (2008) 273–283.
[46] K. Page, Photocatalytic thin films: their characterisation and antimicrobial properties, PhD thesis, UCL, 2009.
[47] P. Wu, R. Xie, J.K. Shang, Enhanced visible-light photocatalytic disinfection of bacterial spores by palladium-modified nitrogen-doped titanium oxide, J. Am. Ceram. Soc. 91 (2008) 2957–2962.
[48] K. Page, R.G. Palgrave, I.P. Parkin, M. Wilson, S.L.P. Savin, A.V. Chadwick, Titania and silver-titania composite films on glass-potent antimicrobial coatings, J. Mater. Chem. 17 (2007) 95–104.
[49] M. Kawashita, S. Tsuneyama, F. Miyaji, T. Kokubo, H. Kozuka, K. Yamamoto, Antibacterial silver-containing silica glass prepared by sol–gel method, Biomaterials 21 (2000) 393–398.
[50] B.S. Atiyeh, M. Costagliola, S.N. Hayek, S.A. Dibo, Effect of silver on burn wound infection control and healing: review of the literature, Burns 33 (2007) 139–148.
[51] A. Mills, J. Wang, Simultaneous monitoring of the destruction of stearic acid and generation of carbon dioxide by self-cleaning semiconductor photocatalytic films, J. Photochem. Photobiol. A: Chem. 182 (2006) 181–186.
[52] Last accessed at http://www.instrumentglasses.com/uv_filter.html.
[53] I. Paramasivam, J.M. Macak, A. Ghicov, P. Schmuki, Enhanced photochromism of Ag loaded self-organized TiO_2 nanotube layers, Chem. Phys. Lett. 445 (2007) 233–237.
[54] I. Paramasivam, J.M. Macak, P. Schmuki, Photocatalytic activity of TiO_2 nanotube layers loaded with Ag and Au nanoparticles, Electrochem. Commun. 10 (2008) 71–75.
[55] Y. Ohko, T. Tatsuma, T. Fujii, K. Naoi, C. Niwa, Y. Kubota, A. Fujishima, Multicolour photochromism of TiO_2 films loaded with silver nanoparticles, Nat. Mater. 2 (2003) 29–31.
[56] B. Ohtani, Y. Okugawa, S. Nishimoto, T. Kagiya, J. Phys. Chem. 91 (1987) 3550–3555.
[57] A. Fernández, A.R. González-Elipe, "In situ" XPS study of the photoassisted reduction of noble-metal cations on TiO_2, Appl. Surf. Sci. 69 (1993) 285–289.
[58] R. Jin, Y. cao, C.A. Mirkin, K.L. Kelly, G.C. Schatz, J.G. Zheng, Science 294 (2001) 1901–1903.
[59] J.J. Mock, M. Barbic, D.R. Mith, D.A. Schultz, S. Schultz, J. Chem. Phys. 116 (2002) 6755–6759.
[60] A. Kafizas, Silver TiO_2 paper, PCCP, 2010.
[61] R. Swanepoel, J. Phys. E 16 (1983) 1214.
[62] J. Tauc, Optical properties and electronic structure of amorphous Ge and Si, Mater. Res. Bull. 3 (1968) 37–46.
[63] J. Tauc, Absorption edge and internal electric fields in amorphous semiconductors, Mater. Res. Bull. 5 (1970) 721–729.
[64] N.R.C. Raju, et al., Physical properties of silver oxide thin films by pulsed laser deposition: effect of oxygen pressure during growth, J. Phys. D: Appl. Phys. 42 (2009) 135411.
[65] Y. Ida, S. Watase, T. Shinagawa, M. Watanabe, M. Chigane, M. Inaba, A. Tasaka, M. Izaki, Direct electrodeposition of 1.46 eV bandgap silver(I) oxide semiconductor films by electrogenerated acid, Chem. Mater. 20 (2008) 1254–1256.
[66] T. Zubkov, D. Stahl, T.L. Thompson, D. Panayotov, O. Diwald, J.T. Yates, Ultraviolet light-induced hydrophilicity effect on TiO_2(1 1 0)(1Ã—1). Dominant role

of the photooxidation of adsorbed hydrocarbons causing wetting by water droplets, J. Phys. Chem. B 109 (2005) 15454–15462.
[67] A. Mills, G. Hill, S. Bhopal, I.P. Parkin, S.A. O'Neill, Thick titanium dioxide films for semiconductor photocatalysis, J. Photochem. Photobiol. A: Chem. 160 (2003) 185–194.
[68] A.B.D. Cassie, S. Baxter, Trans. Faraday Soc. 40 (1944) 546.
[69] R.N. Wenzel, Ind. Eng. Chem. (1936) 988.
[70] Technical publication for the 2D series lamp. Last accessed http://www.gelighting.com/eu/resources/literature_library/prod_tech_pub/downloads/biax2d_datasheet_0506.pdf (April 2010).
[71] R. Beranek, H. Kisch, Electrochem. Commun. 9 (2007) 761–766.
[72] N. Narband, M. Uppal, C.W. Dunnill, G. Hyett, M. Wilson, I.P. Parkin, The interaction between gold nanoparticles and cationic and anionic dyes: enhanced UV–visible absorption, Phys. Chem. Chem. Phys. 11 (2009) 10513–10518.